SOME ELECTRICAL MEASUREMENTS OF MOTONEURON PARAMETERS

P. G. NELSON *and* H. D. LUX

From the National Institute of Neurological Diseases and Stroke, National Institutes of Health, Bethesda, Maryland 20014 and the Deutsche Forschungs Anstalt fur Psychiatrie, Max-Planck Institute, Munich, Germany. Dr. Nelson's present address is the National Institute of Child Health and Human Development, National Institutes of Health, Bethesda, Maryland 20014.

ABSTRACT Electrical properties of the membrane of cat spinal motoneurons have been studied using pulses of current and sinusoidally varying currents applied with intracellular microelectrodes. Hyperpolarization of the motoneuron membrane produces time and voltage dependent changes in membrane resistance and E. M. F. The voltage transients produced by steps of current have been analyzed in order to determine the effective electrotonic length of the dendrites. In a sample of 16 motoneurons, the average total length of the dendrites was 1.5 times the electrotonic length constant of the dendrites. The phase relationship between applied sinusoidal currents and the resultant transmembrane voltage was studied to determine the dendritic to somatic conductance ratio, ρ. In a sample of seven cells the best estimate for ρ was in the range between 5 and 10.

INTRODUCTION

Numerous studies have been made of the electrical properties of neurons in the mammalian central nervous system using techniques of intracellular recording and stimulation (Coombs et al., 1959; Coombs et al., 1955; Creutzfeldt et al., 1964; Eccles, 1961; Frank and Fuortes, 1956; Ito and Oshima, 1965; Lux and Pollen, 1966; Nelson and Frank, 1967; Smith et al., 1967; Spencer and Kandel, 1961). Most of these studies have interpreted the experimental results from the standpoint of a simplified, single time-constant equivalent circuit, although time and voltage dependent membrane properties have been considered in some analyses (Eccles, 1961; Ito and Oshima, 1965; Nelson and Frank, 1967; Smith et al., 1967; Spencer and Kandel, 1961; Takahashi, 1965). In addition to these complications with regard to motoneuronal membrane properties, the importance of the dendritic tree has been emphasized as a determinant of the electrical behavior of neurons (Rall, 1959 *a*, *b*; 1960; 1962 *a*, *b*; 1964; 1967; 1969; Rall et al., 1967).

The present paper provides some additional description of the time, voltage, and current dependence of the changes that have been demonstrated to occur in moto-

neuronal membrane conductance. These changes will be taken into account while using a linear model (Rall, 1969) to get at two questions. (*a*) What are the relative contributions of the cell soma and dendrites to the steady-state conductance of the motoneuron? That is, what is the ratio of the steady-state dendritic conductance to the somatic conductance? (*b*) How far, electrically, are the distal dendrites from the cell soma?

Two analytical and experimental methods have been used. One involves passing steps of current across the neuron membrane with an intracellular electrode and measuring the transmembrane voltage transient produced by this step of current. The other approach utilizes sinusoidally varying currents with measurement of the phase relationship between the current passed across the membrane, and the voltage produced by the current (Falk and Fatt, 1964; Freygang et al., 1967; Lux, 1967).

The results indicate that (*a*) motoneuronal membrane resistance may be time and voltage dependent over a range of membrane hyperpolarization in the vicinity of the resting membrane potential. (*b*) The dendrites may represent 80–90% of the input conductance of the neuron. (*c*) The equivalent length of the dendritic tree is less than two times the equivalent characteristic electrical length of the dendrite.

METHODS

A variety of types of electrodes were used. In some of the experiments involving intracellular injection of steps of current single barreled or double barreled Theta (θ) electrodes were arranged in a bridge circuit as described in a previous paper (Nelson and Frank, 1967). In other experiments of this type double parallel electrodes were used (see below). No electrical cross neutralization of the capacitive coupling between the double Theta electrodes was attempted in these experiments. The extent of the capacitive coupling between electrodes as measured when the electrodes were extracellularly located is indicated in the relevant figures. No attempt has been made to compensate for this coupling by graphical subtraction of intra- and extra-cellular records. It is believed that the variable nature of this coupling makes such a procedure unwarranted. The effect on the analysis of such capacitive artefacts is discussed.

More elaborate double electrodes were necessary for the AC phase angle measurements. Single microelectrodes were bent and coated with a thin layer of silver to within 50–100 μ of the tip. The silver layer was then covered with a thin coat of insulating material. Two such electrodes were positioned so that the final tapering parts (3–4 mm) of the electrodes were parallel and the tips were within 5–10 μ of one another. The pair of electrodes was fastened together with insulating plastic material. Careful adjustment of tip separation was essential to obtain minimal electrical coupling between the electrodes while allowing insertion of both of the electrodes into single motoneurons. Fig. 1 *A* shows identical spikes recorded by both electrodes of such a pair with the very small coupling between them shown when constant current pulses were injected separately through the two electrodes. Cross-neutralization of residual capacitive coupling between the electrodes was accomplished by capacitively coupled phase-inverting amplifiers between the two electrodes in some experiments. This neutralization was adjusted in other experiments by varying the high pass filter at the input of amplifier A_8 of Fig. 1 *B* and by varying the gain of A_3. This compensation for the electrode cross talk was done with the electrode extracellularly located in the motoneuronal pool of the ventral horn before an expected penetration. We may have undercompensated for the interelectrode ca-

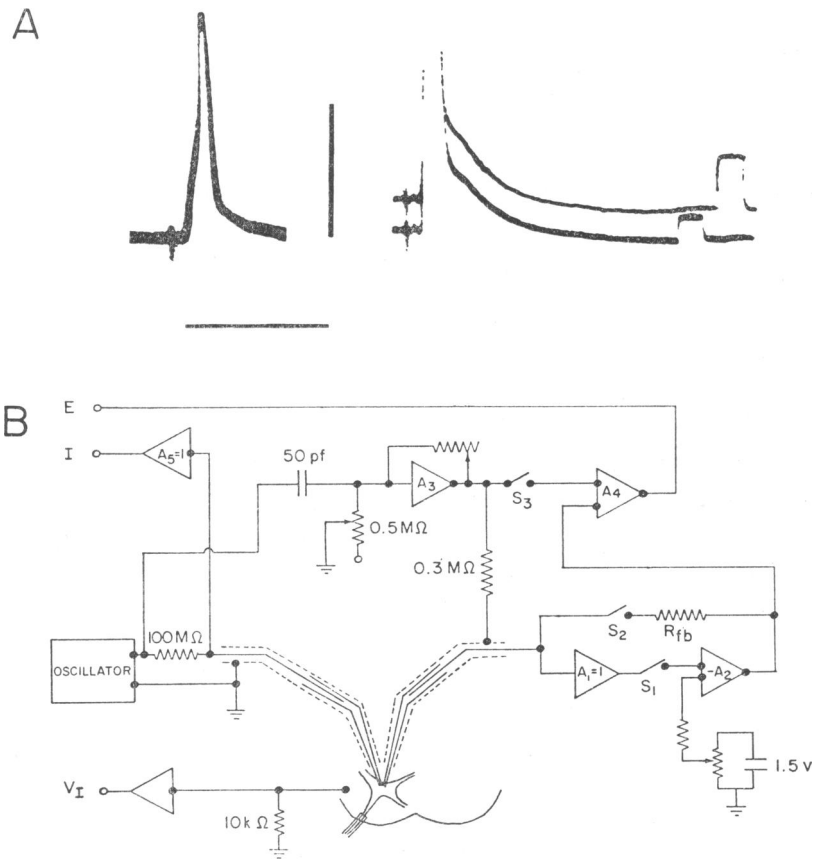

FIGURE 1 *A* Left, essentially identical superimposed action potentials recorded simultaneously with each of two separated electrodes. Right, separate constant current pulses were delivered to the two electrodes near the end of the traces to show degree of coupling between the electrodes. Vertical calibration bar represents 50 mv on left and 10 mv on right. Horizontal bar represents 10 msec in both.

B Block diagram of the circuitry used in the phase angle measurements. The arrangements. The arrangement is closely similar to that described and analyzed in detail by Freygang et al., (1967). A_1 and A_5 are capacity neutralized unity gain amplifiers. Amplifier A_2 was a 702A manufactured by Fairchild Camera and Instrument Corp., Syosset, N. Y.

pacity with respect to that required when the electrodes were intracellular. The cell membrane resistance will remove the electrode system farther from ground and this increases the voltage changes on the electrode tips and, correspondingly, the capacitive electrode coupling (or the effect of the interelectrode capacitance). This error, however, was found to be of importance for frequencies higher (greater than $\omega = 10{,}000$) than those used in the present experiments. No attempt has been made, therefore, to make corrections of the observed phase angle measurements.

Small currents and voltages (5 mv or less) were used in these phase angle measurements in order to minimize distortions due to possible voltage dependent changes in membrane proper-

ties. In some experiments a system of "clamping" the voltage electrode was used as described by Freygang et al. (1967). Closure of switches S_1 and S_2 of Fig. 1 *B* accomplished this. This method was used in order to minimize the effect of stray capacitances between the voltage electrode and ground.

Phase angle measurements were either made directly with a type 40SL phase angle meter (Ad-Yu Electronics, Inc., Passaic, N. J.) or from the Lissajou figures formed by applying signals proportional to current and voltage to the y and x plates, respectively, of a Tektronix 502 oscilloscope (Tektronix, Inc., Beaverton, Ore.). The phase angle between the applied current and the resultant voltage was evaluated from the relationship $\sin \psi = a/b$ where a is the horizontal middiameter of the Lissajou figure and b is the maximum horizontal extent of the Lissajou figure (see Fig. 10).

RESULTS

Voltage Transient Response to Current Pulse

As Ito and Oshima have shown (1965), many motoneurons exhibit time and voltage dependent changes in their membrane properties (even for subthreshold perturbation of membrane potential). Figs. 2 and 3 illustrate some aspects of these nonlinear properties. The term "nonlinear" will refer to situations in which the voltage change elicited by two current pulses delivered together is not the simple summation of the voltage changes produced by the current pulses delivered separately. Steps of current were passed through one barrel of an intracellularly located double pipette and the resultant transmembrane potential measured with the other barrel. A current step sufficient to produce a voltage change of 10 mv or more induced a transient which reached a maximum and then exhibited a "sag" or decrease in amplitude. When the current step returned to zero, a considerable overshoot of the potential past the zero level occurred (Fig. 2 *D*). Furthermore, if a short current pulse was injected during a long pulse of membrane hyperpolarization, the resulting voltage transient was quite different from that occurring in the absence of a long hyperpolarizing pulse. In Fig. 2 *E* the net transients labelled I, II, and III in Fig. 2 *D* are graphically reconstructed. These three transients represent examples that may be compared to determine whether the electrical behavior of the membrane depends on one or more of the following: (*a*) the magnitude of the currents flowing through it, (*b*) the transmembrane voltage, (*c*) the time following a change in membrane voltage. Rall (1960) has provided a theoretical basis for obtaining the true membrane time constant of a neuron with a complex dendritic geometry. With Rall's method the slopes of voltage transients such as those shown in Fig. 2 are measured at various times after the onset of the transient. These slopes are used to construct a graph such as that shown in Fig. 3 in which $\ln(\sqrt{t} \cdot dv/dt)$ is plotted against t. The negative slope of this graph corresponds to the reciprocal of the motoneuron membrane time constant τ_m. This treatment assumes that the dendrites are of unlimited electrotonic length. This assumption is probably not justified (see below), but for purposes of comparison of transients as in the present case, it does not introduce serious

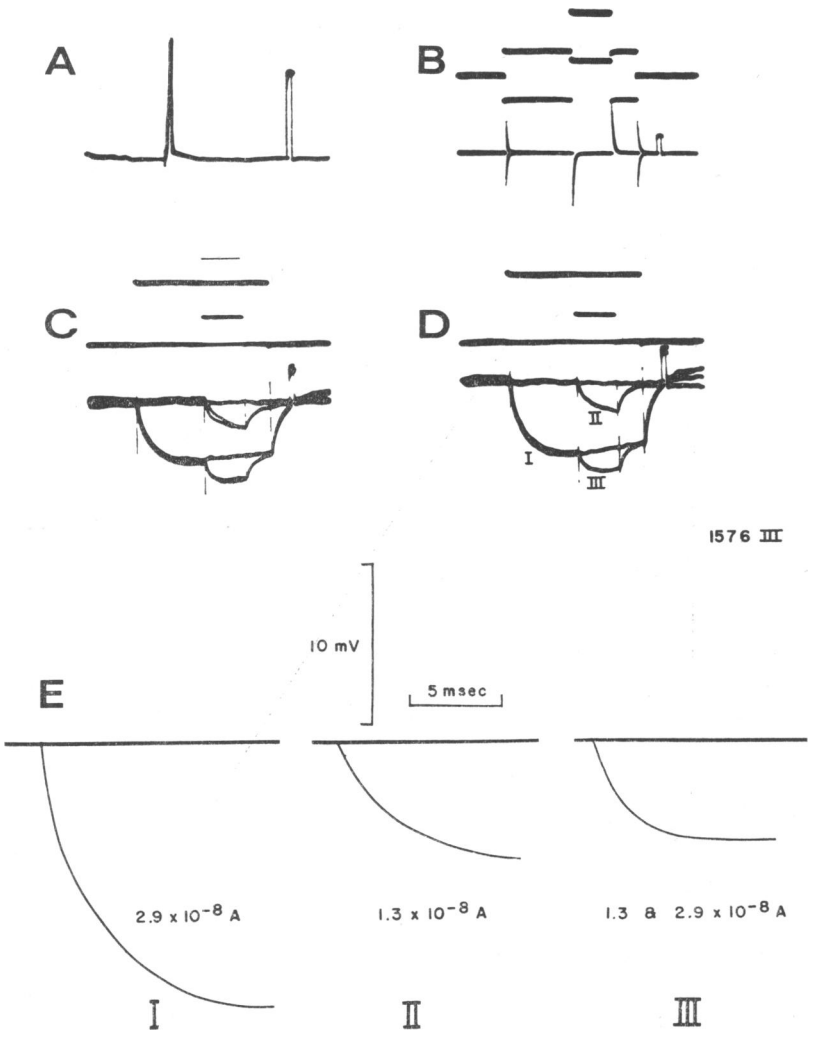

FIGURE 2 *A* Antidromically-evoked action potential. Calibration: 50 mv and 1 msec.

B Records taken after withdrawing the microelectrode from the motoneuron (so that the microelectrode tip is in the extracellular fluid of the spinal cord). Upper traces show the currents that were passed through one barrel of a double microelectrode while the lower traces show the resultant voltages. The calibration pulse at the end of the lower traces represents 10 mv and 1 msec on the voltage trace and 0.7×10^{-8} A on the current trace.

C and *D* Records obtained with the double microelectrode located intracellularly as in *A*. Multiple exposures with no currents, short pulses, long pulses, and long pulses plus short pulses of hyperpolarizing currents being passed across the membrane. Note that in *C* the short pulse of current that is superimposed on the long pulse is just visible on the current record and that in *D* (with a larger, long pulse) the short pulse has gone off the oscilloscope screen. Calibration pulses in *C* and *D* represent 10 mv and 1 msec on voltage trace and 1.5×10^{-8} A on current trace.

E Line drawings of initial portions of the voltage transients in *D*. Those labelled I, II, and III correspond. *E*-III represents the net voltage differences between the voltage elicited by the long current pulse and that developed by the long plus short current pulses. Calibration bars represent, as shown, 10 mv and 5 msec.

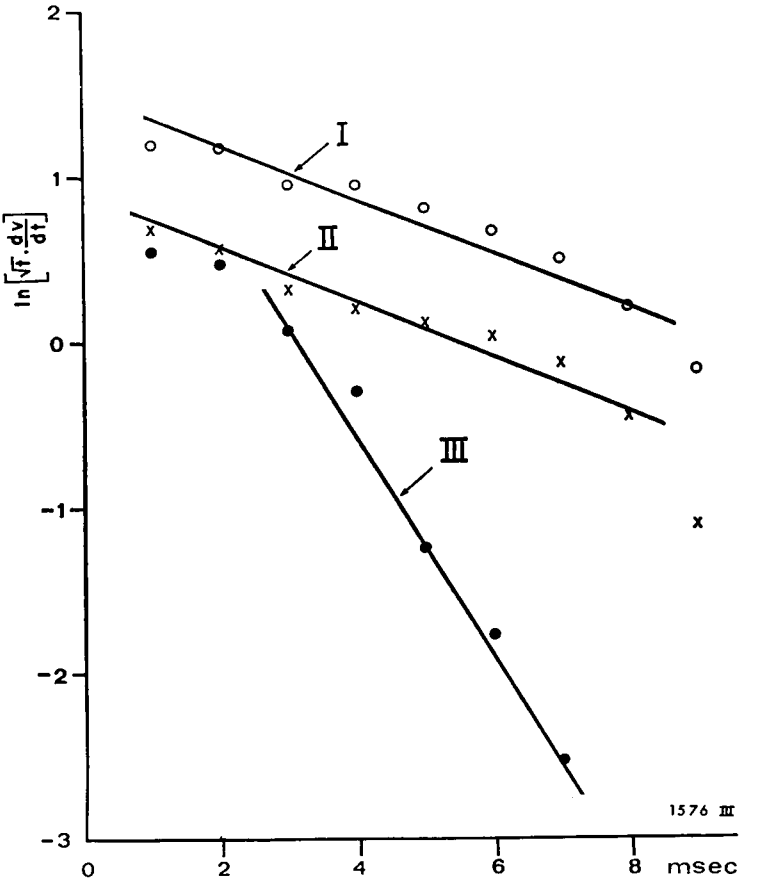

FIGURE 3 Plots for the transients shown in Fig. 2 *E* as labelled.

errors. The slopes of transients I and II are about equal, indicating that the membrane time constant is not affected by variations in the magnitude of the currents and, hence, not by the membrane voltages involved in measuring the time constant if measurements are made soon enough after the onset of the potential change. The slope of the data from curve III, however, is considerably greater than for I and II, indicating that after a membrane potential change has been established for some milliseconds, changes in observed membrane time constant do occur. The alteration in membrane properties is thus both voltage and time dependent.

The change in membrane time constant could be due either to a change in membrane resistivity or E.M.F. or to a change in membrane capacitance. Results shown in Fig. 4 indicate that the change is in the resistive component of the nerve membrane. Pulses of current were injected across the cell membrane in the absence (Fig. 4 *B*) and in the presence (Fig. 4 *C*) of steady hyperpolarizing currents. The decrease in the

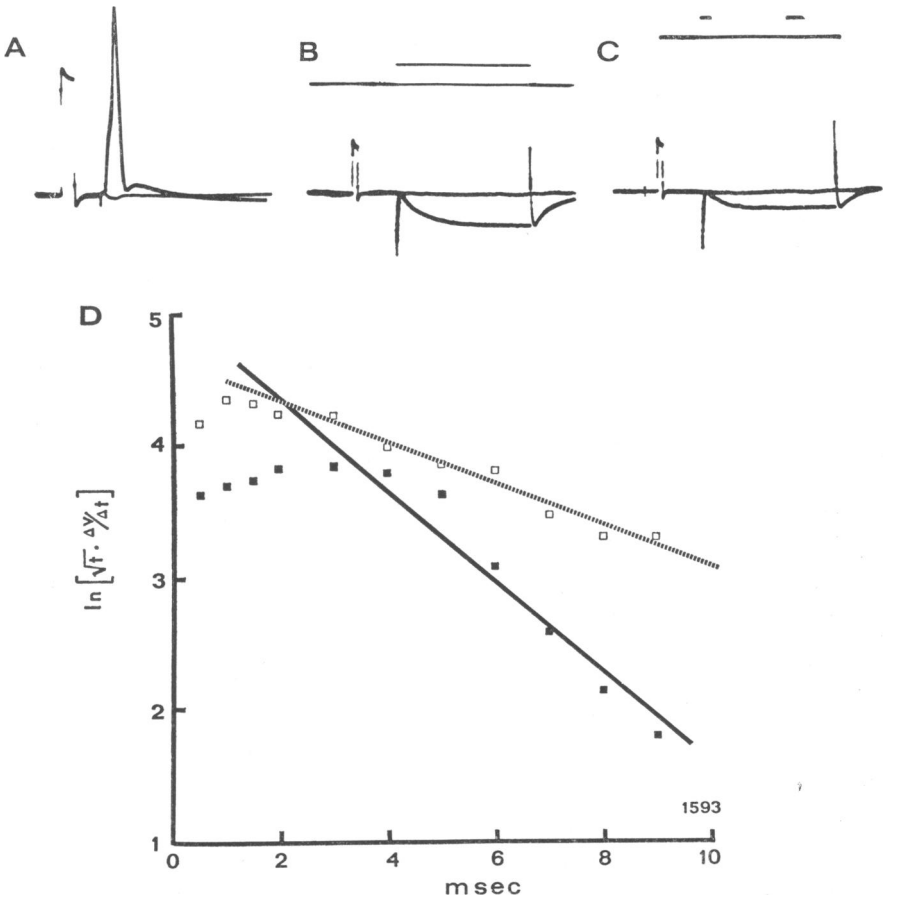

FIGURE 4 *A* Antidromically-elicited action potential. Calibration pulse at beginning of trace represents 50 mv and 1 msec.

B and *C* *Upper trace:* current passed across motoneuron membrane. *Lower trace:* transmembrane voltage developed by that current. Calibration at beginning of voltage trace represents 10 mv and 1 msec in voltage trace and 3.6×10^{-8} A on current trace. Note offset in level of current trace between *B* and *C*, representing passage of steady hyperpolarizing current in *C*. The level of the voltage trace has been compensated at the oscilloscope for the steady change in intracellular potential.

D Plots for membrane potential transients shown in *B* (open squares) and *C* (filled squares).

size of the voltage transient in *C* as compared to *B* indicates that overall cell resistance as measured in 4 *C* is about half that shown in 4 *B*. Similarly the slopes of the plots in 4 *D* indicate that a decrease of about 50% in membrane time constant is produced by the steady hyperpolarizing current. Determination of membrane time constant involves only the early part of the potential transient and it is assumed that no change in membrane properties occurs during the portion of the transient utilized

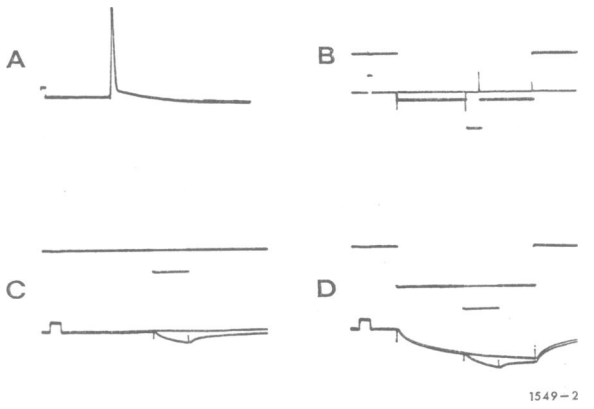

FIGURE 5 *A* Antidromically-elicited motoneuronal action potential. Calibration at beginning of trace represents 10 mv and 1 msec: single microelectrode.

B Records taken with microelectrode located extracellularly. Upper heavy traces record the current and lower trace records the voltage recorded with the microelectrode in a bridge circuit. Calibration pulse on voltage trace represents 10 mv and 1 msec on voltage trace and 0.4×10^{-6} A on current trace.

C and *D* Response recorded intracellularly in same cell as *A*. Upper traces record current; lower traces record voltage. Calibration pulse at beginning of voltage traces represents 10 mv and 1 msec on voltage traces and 0.22×10^{-6} A on current trace. Note the faster time base than in previous records. This cell may well have shown overshoot and sag if longer pulses were used. Since the pulse terminated relatively close to the end of the trace the potential had not returned to the baseline by the end of the trace.

for the analysis. Thus, when hyperpolarizing currents are passed across the cell membrane, an increase in membrane conductance occurs after some time delay. This decrease in R_m with hyperpolarization is in confirmation of previous reports of the presence of anomalous rectification in the motoneuron membrane (Ito and Oshima, 1965; Nelson and Frank, 1967). The time course of the change in conductance will be discussed below.

In some cells this alteration in conductance was not apparent. Records obtained with a single electrode in a bridge circuit are shown in Fig. 5. The linear behavior of the electrode is shown in Fig. 5 *B* with the electrode in the extracellular space. No sag or overshoot in the voltage transient elicited by current pulses is obvious in such cells (Fig. 5 *D*) and there is no marked change in cell resistance, as measured by a short current test pulse, during sustained hyperpolarization. (Compare short voltage transient in center of traces in Fig. 5 *C* and *D*.) This situation of an apparently linear behavior of the membrane is favorable for examining in detail the time course of the voltage transient elicited by a step of current.

Rall (1969) has provided a theoretical basis for relating certain features of such a voltage transient to the linear electrotonic properties of the neuronal dendritic tree. The voltage transient can be shown to be composed of more than one exponential component. This is illustrated in Fig. 6, in which the slope of the transient (at

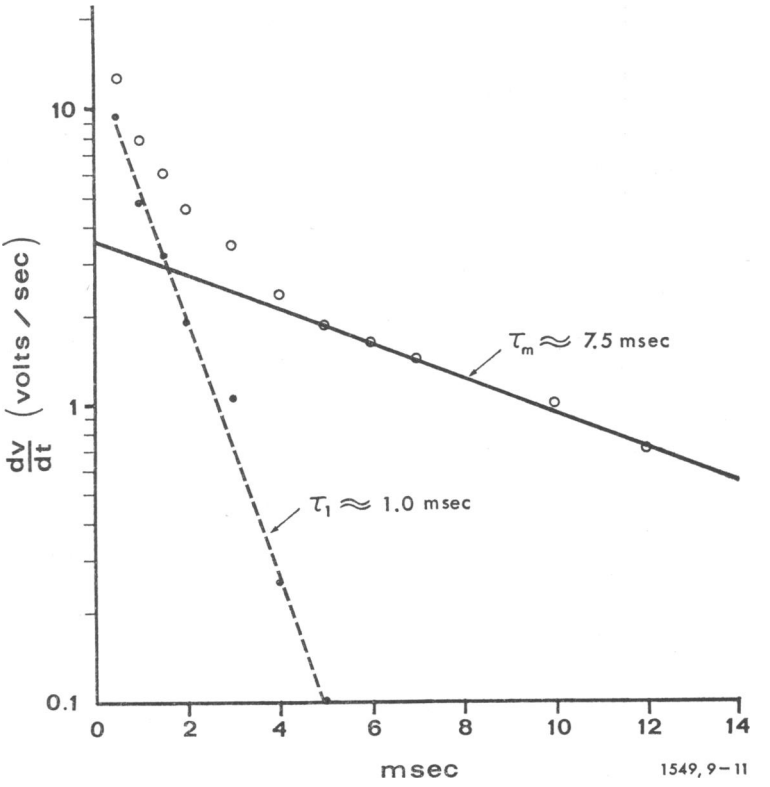

FIGURE 6 Plots of long voltage transients shown in Fig. 5 *D*.

TABLE I
ELECTRICAL CONSTANTS OF MOTONEURONS

	R_n	τ_m	τ_m/τ_1	L
	MΩ	*msec*		
(*a*) n = 7	1.5	3.9	6.3	1.4
Range	(1.0–2.0)	(2.0–7.5)	(5.0–7.5)	
(*b*) n = 9	0.7	4.5	5.1	1.6
Range	(0.4–0.9)	(2.2–8.0)	(2.2–8.9)	
(*c*) Average	1.0	4.2	5.6	1.5

various times after the beginning of the transient) is plotted as a function of time (○). At times greater than 5 or 6 msec, this plot becomes a straight line on semi-logarithmic coordinates as shown in Fig. 6. This late part of the transient would be expected to be an exponential if dendritic length is limited (see Lux, 1967). The time constant associated with the late portion of the plot of Fig. 6 (the time required for dv/dt to decrease by a factor of $1/e$) is, as shown, about 7.5 msec and corresponds to

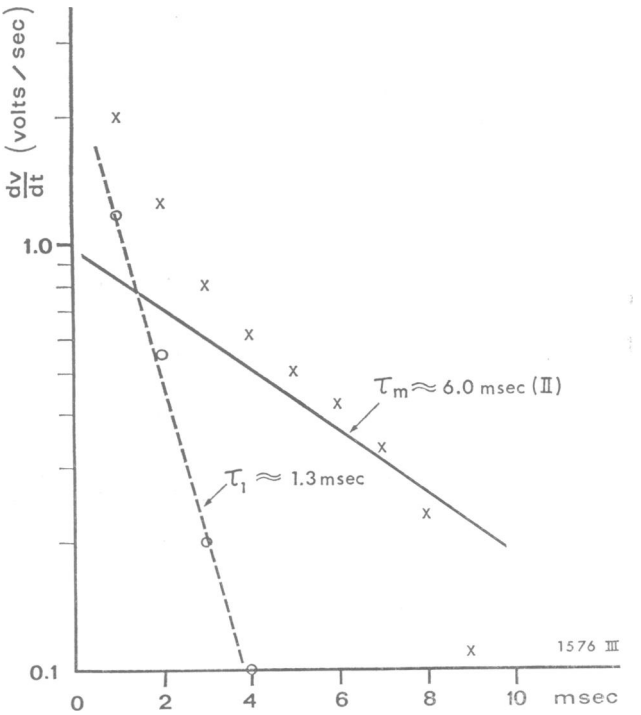

FIGURE 7 Plots of transient II of Fig. 2 *E*.

the time constant of the neuronal membrane. At short times (less than 5 msec) significant deviations from the straight line plot occur. An extrapolation of the straight line portion of the data is given by the solid line. If the differences between this line and the data points are plotted (●), a second straight line plot has a time constant of about 1.0 msec. The data points are thus seen to approximate the summation of two exponential functions. The ratio of the two time constants is related to the total electronic length of the dendrites. In particular Rall (1969) has shown that τ_m/τ_1, $\simeq 1 + (\pi^2/L^2)$, where τ_m equals the longer or membrane time constant, τ_1 represents the "equalizing" time constant characterizing the difference between the data points and the extrapolated τ_m plot, and L equals the total length of the dendrites divided by the equivalent characteristic length of the dendrites.[1]

If the dendritic periphery were only one characteristic length from the neuron soma, the ratio τ_m/τ_1 would be about 10.0. If the dendritic periphery were two characteristic lengths away, the ratio τ_m/τ_1 would be about 3.5. The ratio of 7.5 shown in Fig. 5 corresponds to a total dendritic length of about 1.3 times the characteristic length of the dendrites. In Table I line (*c*) gives a summary of data from 16 cells

[1] Strictly, L corresponds to the total electrotonic length of the equivalent cylinder composed of neuron soma and dendrites. The electrotonic lengths of the dendrites alone are therefore slightly less (by 5–10%) than the L figures given here. With this reservation L will be discussed as the dendritic length.

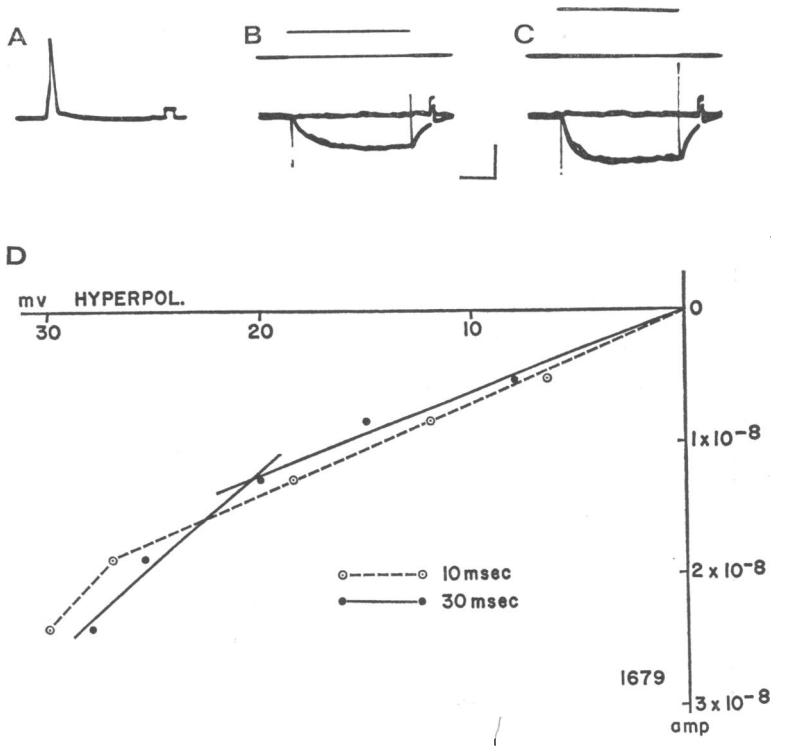

FIGURE 8 *A* Antidromically-elicited action potential. Calibration: 10 mv and 1 msec.

B and *C* *Upper trace:* currents passed through one barrel of double electrode. *Lower trace:* transmembrane voltage recorded with other barrel of microelectrode. Calibration bars between *B* and *C* represent 10 msec and 20 mv on voltage traces and the current pulses in *B* and *C* are 1.2 and 2.2 $\times$ 10^{-8} A, respectively.

D Current vs. voltage plots of data such as that in *B* and *C*. Voltage was measured at 10 msec (dashed line) and 30 msec (solid line) after onset of the pulse.

listing neuron resistance, membrane time constant, τ_m/τ_1, and dendritic electrotonic length. The average τ_m/τ_1 value of 5.6 corresponds to an average total dendritic electrotonic length of 1.5 times the dendritic characteristic length. (See Rall, 1962, 1967, 1969 for a detailed treatment of dendritic characteristic length and total electrotonic length.)

It is clear that the membrane nonlinearities demonstrated earlier could markedly affect the results of an analysis such as that shown in Figs. 5 and 6. When the data in Fig. 2 (curve II) are plotted as dv/dt vs. time, the graph shown in Fig. 7 is obtained. The solid line corresponds to a membrane time constant of 6.0 msec, as was obtained with the ln ($\sqrt{t}.dv \cdot dt$) vs. t plot of Fig. 3. It can be seen that while the data points ($\times$) approach the solid line up to about 7 msec, the points at 8 and 9 msec fall considerably below the line. This effect of the increase in membrane conductance with hyperpolarization can be analyzed in more detail with respect to the data shown in Figs. 8 and 9. Here traces of current and voltage transients are shown

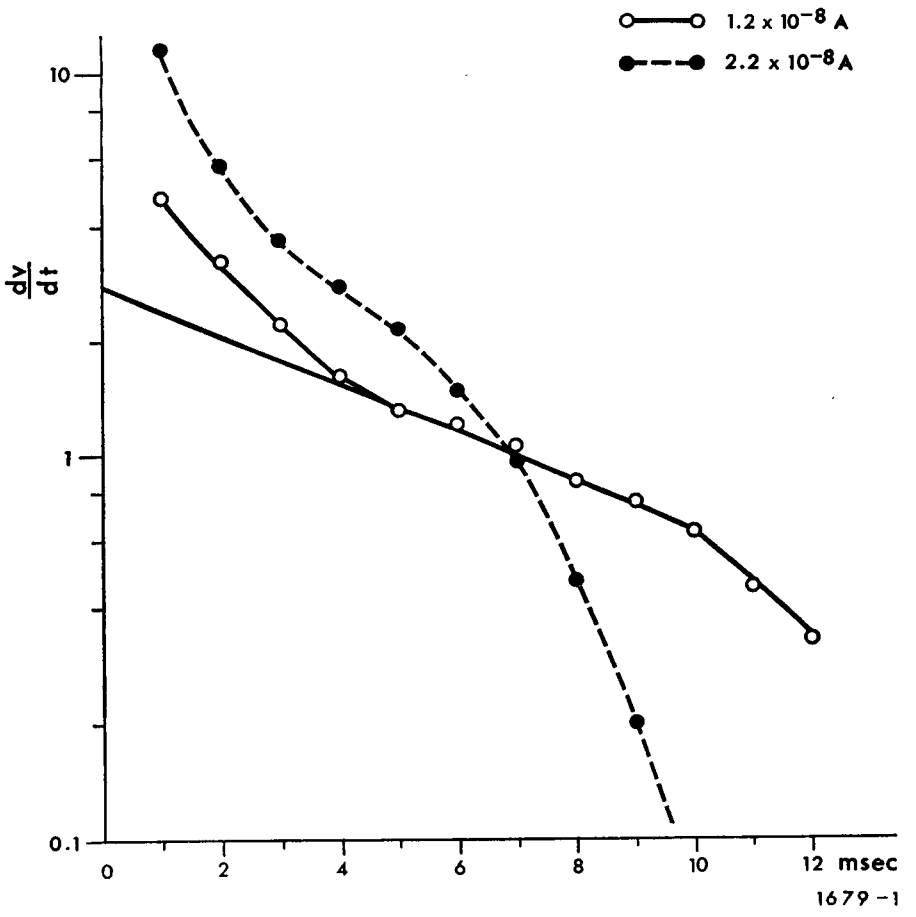

FIGURE 9 Plots of voltage transients shown in Fig. 8 *B* and *C*. The slope measurements were made on the voltage transients elicited by current pulses of two different intensities as shown.

along with plots of current and voltage (Fig. 8). A fall in membrane resistance occurs with membrane hyperpolarization and this is more marked late (●) than early (⊙) in the voltage transients. Values of dv/dt are plotted as a function of t for the voltage transients elicited by two different strengths of current pulses in Fig. 9. For the lesser current pulse, there is relatively little sag or overshoot and only very late in the pulse does any deviation from the straight line portion of the dv/dt vs. t plot appear. With a stronger polarizing pulse, however, the deviation is seen much earlier. For very small currents essentially linear behavior of the membrane is seen. It may be emphasized again that these nonlinearities are all with membrane hyperpolarization and neither local spike-like responses or delayed rectification are involved.

In a sample of 16 cells, no difference between the τ_m/τ_1 values was seen in high resistance as compared to low resistance cells. This is shown in Table I, lines (*a*) and

(*b*), in which cells are divided into those with R_n values less or more than 1 $M\Omega$. In an extensive study involving slightly different techniques, similar τ_m/τ_1 ratios (hence total dendritic electrotonic length) were obtained (Burke, personal communication) with no systematic variation in τ_m/τ_1 as a function of cell resistance or τ_m.

If the data in Table I are analyzed according to the assumptions and method of Lux (1967), a value of about one is obtained for L. The boundary condition for the ends of the dendrites in Lux's analysis was chosen as corresponding to a short circuit across the dendritic terminal membrane. This boundary condition in the model of Rall corresponds to an open circuit at the dendritic termination (sealed-end condition). For either of these boundary conditions, therefore, the analysis of the potential transients indicates a total electrotonic length of 1.5 characteristic lengths or less.

Phase Angle Measurements

An important parameter of the dendritic model of the neuron is the ratio (ρ) of the dendritic input conductance (as seen from the soma) to the somatic surface conductance. ρ can be taken as a measure of dendritic dominance. (For a detailed description see Rall, 1960.)

Determining ρ from the membrane transients elicited by a current step was not found to be practical. This is especially true if ρ's greater than approximately 10 are to be expected. Theoretically, the transient step or pulse responses for ρ greater than one appear quite similar to the response in an infinite cylinder (Lux, 1967, Fig. 2). For this reason AC admittance measurements were performed which permit a more direct insight into the linear electrical properties in such a complex situation as a neuron with dendritic arborizations. The experiments consisted of measuring the phase angle of the distributed impedance when a sine wave input current was compared with the resulting voltage generated across the motoneuron membrane. To reduce interelectrode cross talk, only shielded and separated microelectrodes were employed in making these measurements.

Within the frequency region used (in most cases 2 to *circa* 1000 Hz), the frequency-phase lag curves showed a continuous increase of voltage phase lag from 0–90° with increasing frequencies. No example has been found of an intermediate decrease of phase with increasing frequencies. Such "saddling" has been demonstrated in striated muscle fibers (Falk and Fatt, 1964; Freygang et al., 1967), where it has been attributed to a series capacitance arrangement due to the muscle fiber tubular system. A similarly situated capacitance was postulated by Ito and Oshima (1965) in motoneurons.

We have attempted to determine the values for the parameter ρ, by matching the experimental phase angle versus frequency plots with the theoretical plots of Rall (1960, Fig. 5). Fig. 10 illustrates the difficulty in making such a match; the fit between data points and the theoretical curves varies with frequency. At lower frequencies the data indicate a ρ of 12 while at higher frequencies the data fit with pre-

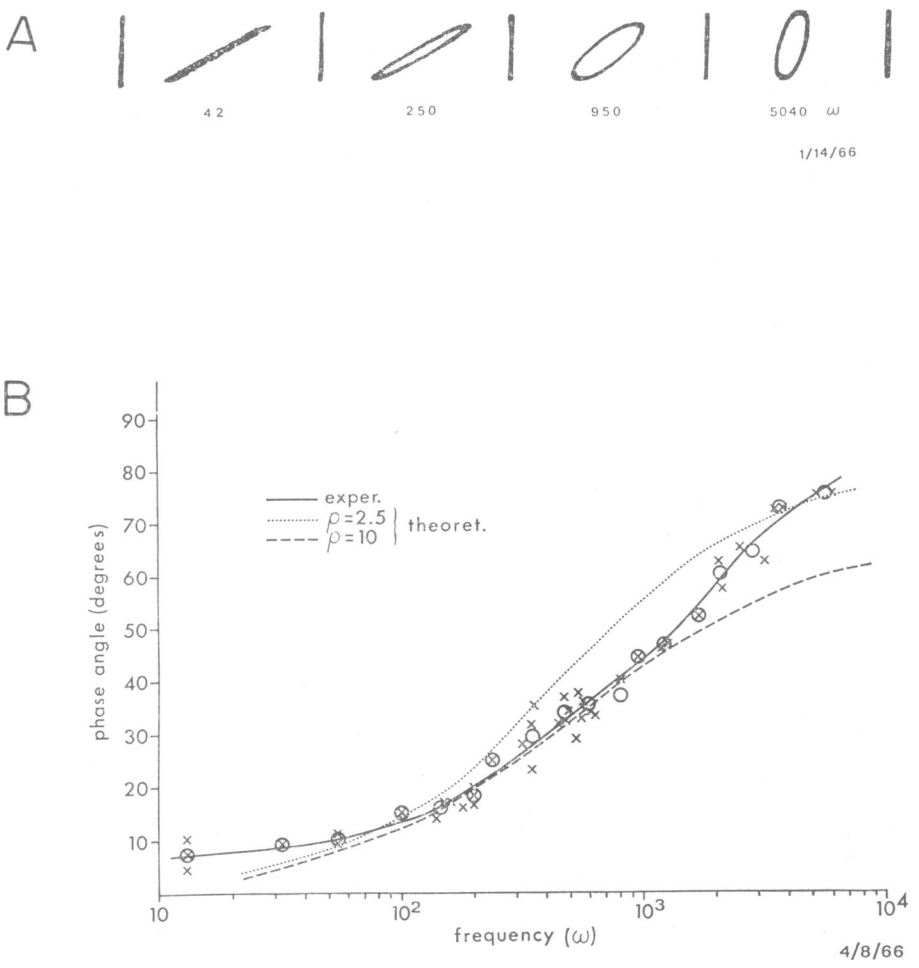

FIGURE 10 *A* Lissajou figures obtained by recording sinusoidally applied current and the resultant voltage on the *y* and *x* plates, respectively, of a Tektronix 502 Oscilloscope. Voltage is ±3 mv in the tracing where $\omega = 42$. (Frequencies are given below each elipse.) The vertical bars separating the Lissajou figures are the results when comparable frequencies were passed with the electrodes located extracellularly, and give an indication of the coupling between the double electrodes. Phase angles, ψ, were evaluated by measuring the horizontal diameter through the midpoint of the elipse, *a*, and the maximal horizontal extension of the elipse, *b*; $\text{Sin}\,\psi$ then equals a/b.

B Phase angle versus frequency plot obtained with a double electrode intracellularly located in a motoneuron (circles, crosses, and solid line). Dotted and dashed lines show expected phase angle-frequency relations for a neuron with a dendritic to soma conductance ratio of 2.5 and 10; respectively. These curves are calculated with the assumption of infinite dendritic length.

dicted values for a ρ of 3. In another cell the data indicated a ρ of 14 for an angular frequency of 250 and a ρ of 6 for an ω of 2500. Table II gives time constant and phase angle measurements at two different frequencies for seven cells, and, for a compari-

TABLE II

EXPERIMENTAL AND THEORETICAL PHASE ANGLES FOR TWO DIFFERENT FREQUENCIES OF APPLIED SINUSOIDAL CURRENTS

Cell No.	Experimental		
	τ_m *msec*	ψ (Phase angle in degrees) $\omega\tau = 1$	$\omega\tau = 10$
1/14/66	3.0	23	53
1/27/66	2.7	22	54
2/8/66	2.2	22	55
3/22/66	4.5	28	53
3/25/66	3.0	28	64
4/8/66	3.8	25	63
12/28/66 *a*	3.4	27	61
12/28/66 *b*	1.9	26	62
Average	3.1	25	58
	Theoretical		
$\rho = 2.5$		30	66
$\rho = 10$		25	52
$\rho = 20$		23	47

son, the theoretically predicted phase angles for different ρ according to the method of Rall (1960).

It is clear that no one value of ρ gives theoretical phase angle values corresponding to the experimentally observed phase angles for both values of $\omega\tau$. The experimental phase vs. frequency plots in the medium frequency range ($\omega = 100$ to $\omega = 1000$) would be in accordance with ρ values $\simeq 10$ but obvious deviations are shown in the higher frequency range. Thus a ρ of 10 would be indicated by the experimentally obtained ψ of 25° at $\omega\tau$ equal to one while the experimental ψ of 58° at $\omega\tau$ of 10 corresponds to a predicted ρ between 2.5 and 10. Two factors require consideration in evaluating these results. (*a*) The theoretical method of computing ρ as a function of ψ involves the assumption of dendrites of infinite electrotonic length ($L = \infty$). A theoretical consideration of the effect of this assumption as to dendritic length indicates the predicted ρ values are not strongly affected (Rall, personal communication). Calculations made on the assumption of dendrites of finite length do not give results materially different from those shown in Fig. 10 and are in no closer agreement to these experimental phase versus frequency plots. (*b*) Interelectrode resistive and capacitive coupling can not be completely eliminated and can be compensated for only imperfectly. As a result of this, the experimental determination could be too high by as much as 5–10 degrees, especially in the higher frequency region. If this relatively greater error at higher frequencies is taken into account, the discrepancy between the observed phase angle of 58 for $\omega\tau = 10$ and the predicted value of 52 for a ρ of 10 becomes diminished. The discrepancy between observed values and predicted values for a value of $\rho = 2.5$ is increased when possible instrumental errors

are taken into account. The observed phase angle of 58 degrees for $\omega\tau = 10$ corresponds to that predicted for a ρ of 5. Thus, despite the lack of a perfect correspondence between the observed phase angle measurements and those predicted on the basis of a unique value for ρ, a range of possible ρ values between 5 and 10 seems justified.

The determination of ρ was not dependent on the specific value of membrane time constant. This was shown in cell 12/28/66 in which measurements were made in the absence and in the presence of steady hyperpolarizing current. At resting membrane potential the cell time constant was 3.4 msec while during hyperpolarization the time constant dropped to 1.9 msec. The phase angle measurements changed correspondingly so that when expressed in terms of $\omega\tau$ the results were comparable for resting and hyperpolarized conditions.

DISCUSSION

Membrane Current-Voltage Relations

The experiments, described above, dealing with the injection of pulse and steady currents across the motoneuron membrane indicate that this membrane does not, in general, exhibit linear electrical properties. The nature of this nonlinearity may be summarized as follows.

1. If steady-state voltage is plotted as a function of polarizing current, a nonlinear relationship is found in many motoneurons (Ito and Oshima, 1965; Nelson and Frank, 1967; and Fig. 8 of present paper). (This is true even when considering only hyperpolarization of the membrane).
2. When brief, small test pulses of current are superimposed on steady currents, membrane time constant and resistance are both shown to be decreased by hyperpolarization.
3. When steps of current are passed across the membrane, the voltage transient sometimes exhibits an early maximum with subsequent decrease or sag. On turning off a current step an overshoot occurs past the resting membrane potential (Araki et al., 1962; Nelson and Frank, 1967; and Fig. 2 of present paper). These phenomena are seen both for hyperpolarizing and depolarizing pulses. While the effects in some cells may be reasonably symmetrical (Araki et al., 1962) in others both the sag and overshoot are different for depolarizing and hyperpolarizing pulses. The degrees of sag and overshoot are strongly affected by changes in membrane potential (Ito and Oshima, 1965, Table I; and results of the present investigation, not illustrated).
4. This nonlinearity is not present in all cells. Ito and Oshima, in general using smaller test currents than those used in the present study, observed membrane potential overshoots, sags, and undershoots and successfully analyzed these in terms of a linear membrane model involving three exponential processes. Close correlation was seen between the voltage changes and excitability changes in the

impaled cells. For small perturbations of the membrane potential, therefore, processes other than changes in membrane conductance may be responsible for the sag and overshoot phenomena. However, in some cells, membrane conductance changes continuously with membrane potential around the resting potential (Ito and Oshima, 1965, Fig. 13; Nelson and Frank, 1967, Fig. 4) and Ito and Oshima describe the general features of the potential changes in their study as "quasi-superpositional." The previous data and those of the present paper indicate that with perturbations of 10 mv or more from resting potential, alterations in membrane conductance may be involved in determining the form of the transients elicited by current injection. The nature of this change and the ions which are involved are not specified by the present experiments.

No correlation has been noted between the presence or absence of membrane nonlinearity and the muscle that a given motoneuron innervates (Nelson and Burke, unpublished results). The functional significance of the nonlinearity is obscure (but see Kandel and Tauc [1966]).

Analysis of Membrane Transients

As reported earlier in abstract form (Lux and Nelson, 1966), time constant measurements have been made on a number of motoneurons using double electrodes (Theta electrodes and shielded double electrodes). An average value of 4.85 $\pm$ 1.55 msec was obtained by using the analysis proposed for a neuron governed by dendrites with unlimited electrotonic lengths (Rall, 1960). Average cell resistance near resting potential was 1.15 $\pm$ 0.25 MΩ. In addition, in the present study, the time constant measurements were useful in demonstrating that a change in cell conductance as well as a change in membrane E.M.F. occurred during hyperpolarization (Figs. 2–4).

Considerable attention has been paid to the manner in which the time course of the conductance increase with hyperpolarization (or any other mechanism which may underly the overshoot and sag) affects the voltage transients elicited by current steps. The membrane time constants measured with currents of different magnitude are closely similar (Figs. 2 and 3), although at the steady state greater changes in membrane conductance are produced by the larger currents. The analysis of the transients discussed below is made on the basis that one can select early portions of the voltage transients under consideration which are not seriously affected by the sag, overshoot, and nonlinearities discussed earlier.

The analysis of the potential transients based upon a model of Rall (1969) involving closed-ended dendrites of finite length has provided a means of determining the total electrotonic length of the dendritic tree. In earlier papers the optimal prediction of EPSP waveforms recorded from motoneurons was obtained by assuming a total dendritic electrotonic length of 1.8 characteristic lengths (Burke, 1967; Rall 1967; Rall et al., 1967). The range of values indicated by that study is quite consistent with the results obtained in the present study. Rall (1967) discusses in detail the

implications of such a dendritic structure with an L of 1–2. For such values of L, to produce a small EPSP measured at the soma, a synaptic input at the dendritic periphery would have to be about ten times as intense as an input close to the soma. For larger EPSP's this disparity would be even greater. Nonetheless, these calculations show that significant potential changes could be produced in the somatic trigger area by synaptic input even in the most distal regions of the dendrites.

In the study by Ito and Oshima (1965), the ratio of the first and second exponentials used by them to characterize the motoneuronal transient response (τ_m and τ_1 in the present study) range from 5–10. These results are very close to those of the present study.

Consideration must be given to possible sources of artefact in the analysis of the potential transients given above. A serious problem is the capacitive artefact which is present whether one uses single or double electrodes. This artefact tends to decrease the steepness of the very early portion of the transient, while affecting later portions of the transient very little. These capacitive artefacts will, therefore, tend to increase the value of τ_1 while leaving τ_m less affected. This will make τ_m/τ_1 smaller and L larger. Thus, this instrumental error is such that the values of L given in Tables I and II are upper limits on the true L. The total electrotonic length of the dendrites might be even less than 1.5 characteristic lengths.

The occurrence of time dependent membrane nonlinearities also complicates the determination of L. This factor tends to decrease τ_m while leaving τ_1 little changed or decreased. The net effect may be complex, but in general, will also tend to decrease τ_m/τ_1 and thus increase L. Again, this has the effect of making the stated value of L serve as an upper limit for this parameter.

Phase Angle Measurements

The AC analysis shows that the part of the applied current flowing into the dendritic conductance is considerably greater than the somatic surface current. We estimate that the conductance ratio (ρ) of the dendritic and the somatic surface is in the range of 5–10, which means that up to 90% of the applied current is flowing through the dendritic membranes. There is no indication of a cell membrane having a more complicated impedance than that of a distributed capacitance and resistance in parallel. From this it appears more likely that the responses to applied AC currents are governed by the geometry of the cells dendritic structure and not by special cell membrane properties.

The range of ρ values as determined electrophysiologically is as stated about 5–10. This is compatible with the available anatomical measurements (Aitken and Bridger, 1960; Mannen, 1966). The conclusion from both types of experiment is that the dendritic tree greatly dominates over the soma as far as the receptive surface of the neuron is concerned.

Received for publication 10 July 1969 and in revised form 4 September 1969.

REFERENCES

AITKEN, J. T., and J. E. BRIDGER. 1960. *J. Anat.* **95**:38.

ARAKI, T., M. ITO, and T. OSHIMA. 1962. *Nature* (*London*). **191**:1104.

BURKE, R. E. 1967. *J. Neurophysiol.* **30**:1114.

COOMBS, J. S., D. R. CURTIS, and J. C. ECCLES. 1959. *J. Physiol.* (*London*). **145**:505.

COOMBS, J. S., J. C. ECCLES, and P. FATT. 1955. *J. Physiol.* (*London*). **130**:291.

CREUTZFELDT, O. D., H. D. LUX, and A. C. NACIMIENTO. 1964. *Pflugers Arch. Gesamte Physiol. Menschen Tiere.* **281**:129.

ECCLES, J. C. 1961. *Exp. Neurol.* **4**:1.

FALK, G., and P. FATT. 1964. *Proc. Roy. Soc. Ser. B Biol. Sci.* **160**:69.

FRANK, K., and M. G. F. FUORTES. 1956. *J. Physiol.* (*London*). **134**:451.

FREYGANG, W. J., JR., S. I. RAPPOPORT, and L. D. PEACHEY. 1967. *J. Gen. Physiol.* **50**:2437.

ITO, M., and T. OSHIMA. 1965. *J. Physiol.* (*London*). **180**:607.

KANDEL, E. R., and L. TAUC. 1966. *J. Physiol.* (*London*). **183**:287.

LUX, H. D. 1967. *Pflugers Arch. Gesamte Physiol. Menschen Tiere.* **297**:238.

LUX, H. D., and P. G. NELSON. 1966. Impedance measurements of cat motoneurons with separated microelectrodes. Abstracts of the Proceedings of the 2nd International Biophysics Congress, Vienna Sept. 5–9, 1966.

LUX, H. D., and D. A. POLLEN. 1966. *J. Neurophysiol.* **29**:207.

MANNEN, H. 1966. *Progr. Brain Res.* **21A**:131.

NELSON, P. G., and K. FRANK. 1967. *J. Neurophysiol.* **30**:1097.

RALL, W. 1959 *a*. Dendritic current distribution and whole neuron properties. Research report of the Naval Medical Research Institute. **NM-01-05-00.01.02**:479.

RALL, W. 1959 *b*. *Exp. Neurol.* **1**:491.

RALL, W. 1960. *Exp. Neurol.* **2**:503.

RALL, W. 1962 *a*. *Ann. N.Y. Acad. Sci.* **96**:1071.

RALL, W. 1962 *b*. *Biophys. J.* 2(2, Pt. 2):146.

RALL, W. 1964. *In* Neural Theory and Modeling. R. F. Reis, editor. Stanford University Press, Stanford. 73.

RALL, W. 1967. *J. Neurophysiol.* **30**:1138.

RALL, W. 1969. *Biophys. J.* **9**:1483.

RALL, W., R. E. BURKE, T. G. SMITH, P. G. NELSON, and K. FRANK. *J. Neurophysiol.* **30**:1072.

SMITH, T. G., R. B. WUERKER, and K. FRANK. 1967. *J. Neurophysiol.* **30**:1072.

SPENCER, W. A., and E. R. KANDEL. 1961. *J. Neurophysiol.* **24**:260.

TAKAHASHI, K. 1965. *J. Neurophysiol.* **28**:908.